



## The Effect of Annealing Temperature on The Structural and Optical Properties of Fe<sub>2</sub>O<sub>3</sub> Thin Films

Mustafa Shakir Hashim

Amira Jawad Kadhim

Esraa Akram Abbas

Reem saadi Khaleel

Physics department, Education College, Almustansiriya University, Iraq.

Received Date: 22 / 11 / 2016

Accepted Date: 19 / 2 / 2019

### الخلاصة

أستخدم الرش الكيميائي الحراري لترسيب أغشية أكسيد الحديد على قواعد زجاجية مُسخَّنة مسبقاً بدرجة (200) °م. لُذَّت العينات بدرجات (300)، (400) و(5000)°م بمحيط جوي. وُظِّفَت تقنية جُيُود الأشعة السينية لدراسة تأثير التلدين على تركيب أغشية أكسيد الحديد. ان تركيب الأغشية المرسبة تركيب عشوائي تحول الى مُتعدد التبلور بالتلدين على درجة (300) °م باتجاه مُتسِّد [104]. تحسَّن التركيب البلوري مع زيادة درجة حرارة التلدين. مع المعاملة الحرارية زاد حجم الحبيبات البلورية النانوية من (23.3) الى (29.3) نانوميتر للغشاء المُرسَّب والمُلْدَّن بدرجة (500) °م على التوالي. مَعْلَمَات تركيبية أخرى كالمطاوعة الميكروية، كثافة الإنخلاعات وعدد الحبيبات البلورية لوحدة المساحة حُسِبَت ورُبِطَت مع تغيرات درجات التلدين. أستمعمل مطياف الأشعة فوق البنفسجية والأشعة المرئية لدراسة تأثير التلدين على الخواص البصرية لا غشية أكسيد الحديد. زادت فجوة الطاقة البصرية مع التلدين من (2.105) الى (2.159) إلكترون فولت نتيجة نقصان الحالات المتموضعة داخل فجوة الطاقة من (0.396) الى (0.162) إلكترون فولت.

### الكلمات المفتاحية

التلدين، Fe<sub>2</sub>O<sub>3</sub>، الحجم الحبيبي، التبلور، فجوة الطاقة، عرض الذبول.



### Abstract

Chemical spray pyrolysis was used to deposit  $\text{Fe}_2\text{O}_3$  thin films on pre-heated glass substrates at  $(200)^\circ\text{C}$ . The films were annealed at  $(300)$ ,  $(400)$  and  $(500)^\circ\text{C}$  at ambient atmosphere. X ray diffraction (XRD) technique was utilized to study the effect of annealing on the structure of  $\text{Fe}_2\text{O}_3$  thin films. XRD technique was utilized to study the effect of annealing temperature on structural properties of  $\text{Fe}_2\text{O}_3$  thin films. It was found that the as deposit thin film has amorphous structure but it became polycrystalline structure by annealing at  $(300)^\circ\text{C}$  with dominant orientation along  $[104]$  direction. with dominant orientation along  $[104]$  direction. Crystallinity of  $\text{Fe}_2\text{O}_3$  thin films was improved with increasing annealing temperature ( $T_a$ ). Crystallite size increased with heat treatment from  $(23.3)$  to  $(29.3)$  nm for as deposit and annealed sample at  $(500)^\circ\text{C}$  respectively. Other structural parameters like micro strain ( $\eta$ ), dislocation density and number of crystallites per unit area were calculated and correlated with the variation of  $T_a$ . UV-Visible spectrophotometer was used to study the annealing effects on optical properties of  $\text{Fe}_2\text{O}_3$  thin films. With increasing of  $T_a$ ; optical energy gap ( $E_g$ ) values increased from  $(2.105)$  to  $(2.159)$  eV due to decreasing of localized states inside the band gap from  $(0.396)$  to  $(0.162)$  eV.

### Keywords

annealing,  $\text{Fe}_2\text{O}_3$ , grain size, crystallinity, energy gap, band tail.



## 1.Introduction:

Transition metal oxide thin films have great interest for their variable applications. Iron oxide is one of these materials with multiple applications [1]. Size reduction alters chemical and physical properties of materials and has intense recent research. Metal oxides with microstructures like nanorods, nanotubes, and nanoparticles as building blocks have been attracted great interest [2]. In applications of thin films field, Iron oxide has several employments. As a result, to its fast response  $\text{Fe}_2\text{O}_3$  thin film is using to sense flammable gas [3]. Due to its high absorption coefficient and small energy gap it is utilized as solar cell [4]. This material is low cost, nontoxic, has environmentally friendly properties, high chemical stability, high corrosion resistance and easy to fabricate [5]. Spray pyrolysis method is a simple, versatile and low cost technique. Large number of different thin films types can prepare by this technique. By this method mixed and doped thin films are deposited [6]. Also without the need of an ultra-high vacuum by using this method it can produce large area films and it can be controlled easily [7]. Annealing process is a simple method utilized to get multiple advantageous for example it is used to improve crystallinity and minimized defects and dislocations.

In this contribution an attempt is done to study the effect of annealing on structural and some optical properties of  $\text{Fe}_2\text{O}_3$  thin film.

## 2.Experimental part:

$\text{Fe}_2\text{O}_3$  thin films deposit on preheated glass

substrates. The best examined conditions of deposition were: substrate temperature (200)  $^{\circ}\text{C}$ , the time of spraying (5) s, distance between substrate and nozzle was (30 $\pm$ 1) cm and carrier gas was filtered air. The used solution consists from  $\text{FeCl}_3 \cdot 6\text{H}_2\text{O}$  (1.6221) g powder as a precursor of Fe dissolved in distilled water (100) ml. To ensure the complete dissolving of powder inside the solution it was left under magnetic stirrer for (30) minute. The thickness of deposit films was determined by weight method; it was (45020 $\pm$ ) nm. Shimadzu X-ray diffractometer is utilized to determine the orientations of  $\text{Fe}_2\text{O}_3$  miller indices. To characterize the optical properties of the samples UV-Visible (1800) spectra photometer is used.

## 3.Results and discussions:

Fig. (1) shows XRD pattern of as deposit and annealed  $\text{Fe}_2\text{O}_3$  thin films. In general; as deposit sample has amorphous structure but there is a beginning to form a peaks along (104) and (110) planes. After annealing the structure transform to polycrystalline with dominant direction at [104] beside several peaks. According to standard card (JCPDS) with number (00033-0664) annealed samples have hexagonal phase. The sharpness of all peaks increases with increasing of Ta.

After annealing at (500)  $^{\circ}\text{C}$ ; the dominant peak (104) becomes sharper and higher intensity. This result attributed to the increasing of sample's crystallization and reduction of defects. The rearrangements of atoms positions inside  $\text{Fe}_2\text{O}_3$  lattice are achieved when Ta reach to (500)  $^{\circ}\text{C}$  [8].

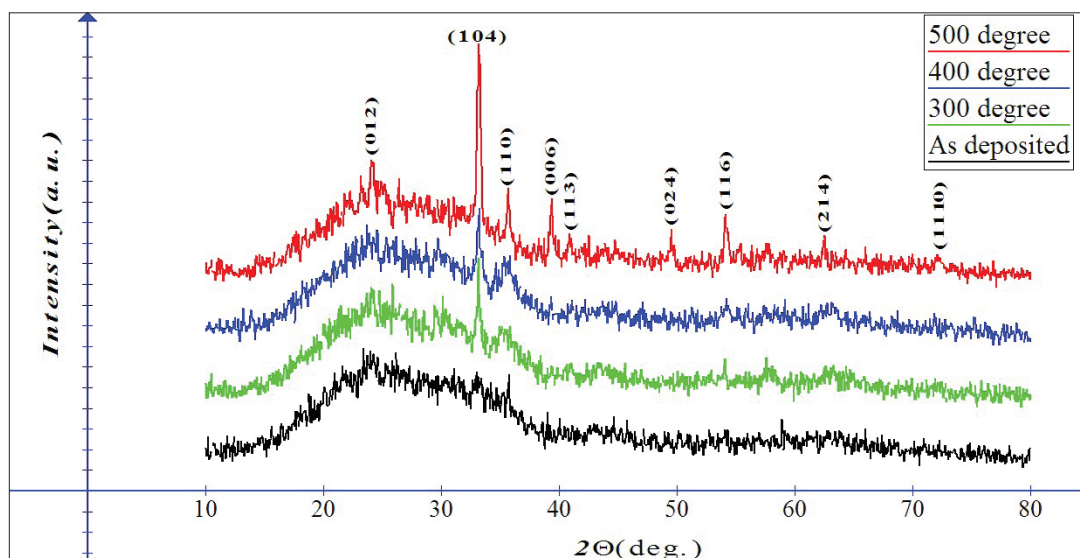


**Fig. (1): XRD of as deposit and annealed samples.**

For (104) peak of standard, as deposit and annealed  $\text{Fe}_2\text{O}_3$  Table 1 shows interplanar spacing ( $d_{hkl}$ ) and peak position ( $2\theta$ ).

**Table (1): (104) peak data at different Ta.**

Sample type	$2\theta$ (degree)	$d_{hkl}$ (Å)	FWHM (radian)
Standard $\text{Fe}_2\text{O}_3$	33.152	2.7	-
As deposit	33.0798	2.70582	0.0076
Annealed at (300) °C	33.1872	2.69731	0.0075
Annealed at (400) °C	33.1897	2.69711	0.0073
Annealed at (500) °C	33.1957	2.69663	0.0061

In comparison with standard value it was found that all annealed samples have shifted positions to right and this shift increases with Ta. On the other hand, the values of interplanar spacing ( $d_{hkl}$ ) for annealed samples are less than that of standard one. The behavior of  $2\theta$  and  $d_{hkl}$  is a direct result to Bragg law. Crystallite size is calculated by using Scherrer's equation [9].

$$\text{Crystallite size}(\xi) = \frac{0.94\lambda}{\beta \cos\theta} \quad (1)$$

Where  $\lambda$  is x-ray wavelength,  $\beta$  is the broadening of the hkl diffraction peak measured at half of its maximum intensity (in radians) and  $\theta$  is Bragg diffraction angle (°). Crystallite size increase with Ta until it reached to (500) °C which it exhibited a maximum size. This result is in agreement with previous reports [10].



Also Fig. (2) illustrates the decreasing of full width at half maximum (FWHM) with Ta indicating to the enhancement of the crystalline quality of the films. It is known that an increase

in Ta leads to an increase in kinetic energy of the atoms and molecules making it easier for them to correct their occupancy in the lattice and then increase the size of the crystallites [8].

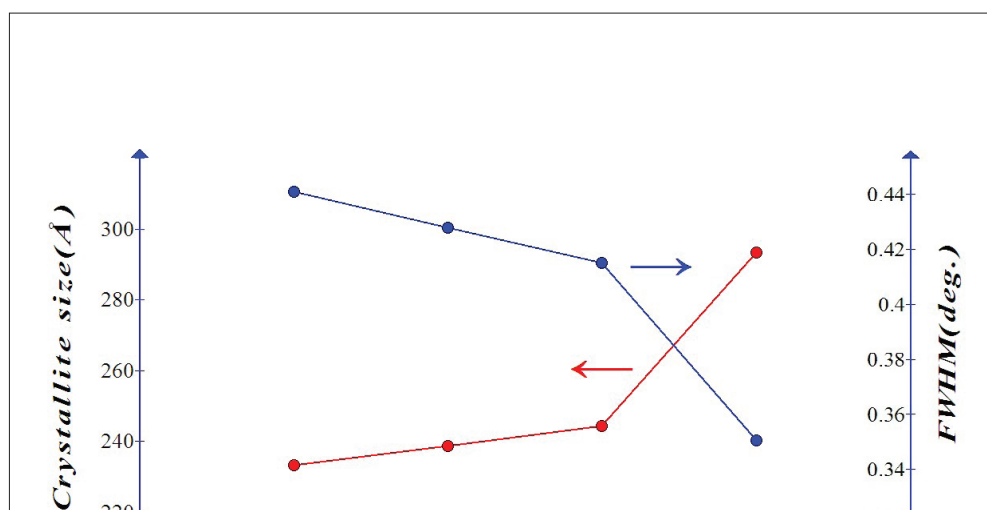


Fig. (2): crystallite size and FWHM as function to Ta.

XRD pattern is utilized again to calculate lattice constants ( $a_0$  and  $c_0$ ) by using equation

$$2 [11]. \quad \frac{1}{d^2} = \frac{4}{3} \left( \frac{h^2 + hk + k^2}{a_0^2} \right) + \frac{l^2}{c_0^2} \quad \text{--- (2)}$$

Where  $h, k, l$  are miller indices. The results of are tabulated in Table 2.

Table (2): Lattice constants for as deposit and annealed samples.

Lattice constant (Å)	Standard (JCPDS)	As deposit	(Ta (°C)		
			300	400	500
$a_0$	5.035	5.04	5.051	5.063	5.027
$c_0$	13.74	13.79	13.70	13.68	13.73

Table (2) confirms the recrystallization of all annealed samples due to the change in  $c_0$  parameter compared with that of as deposit sample. Current lattice constants close to that obtained by Shinde *et al.* [12]. After annealing at (300) and (400) °C ( $a_0$ ) increases but it decreases at (500) °C. ( $c_0$ ) has reverse behavior

as equation (2) impose. For as deposit and annealed samples; Table (3) shows the values of micro strain ( $\eta$ ), dislocation density and number of crystallites per unit area by using equation (3,4 and 5): [8].

$$\eta = \frac{|c_0(JCPDS) - c_0(XRD)|}{c_0(JCPDS)} * 100\% \quad \text{--- (3)}$$



$$N_d = \frac{1}{\xi^2} \text{ --- (4)}$$

$$N_c = \frac{t}{\xi^3} \text{ --- (5)}$$

Where  $t$  is thin film thickness [13].

**Table (3): Some physical parameters of  $\text{Fe}_2\text{O}_3$  thin films**

Sample	Micro strain % ( $\eta$ )	Dislocation density $\times 10^{11}(\text{cm}^{-2})$	Number of crystallites per unit area $\times 10^9(\text{cm}^{-2})$
As deposit	0.36 -	1.83	3.4
Annealed at $(300)^\circ\text{C}$	0.29	1.75	3.6
Annealed at $(400)^\circ\text{C}$	0.43	1.67	2.97
Annealed at $(500)^\circ\text{C}$	0.72	1.16	1.9

A strain can define as following: it is measure of deformation representing the displacement between particles in the body relative to a reference length. For as deposited film non-uniform strain in the films is responsible on broadening in XRD profile, these strain is caused during the growth of thin film [14]. From Table 3 and Fig. (2) it is clear that the increasing of micro strain is related to the increasing of crystallite size which increases with  $T_a$ . This may due to decrease of mechanical surface-free energy with annealing. The dislocation density, defined as the length of dislocation lines per unit volume [15]. Table 3. shows the decreasing of dislocation density with  $T_a$ , the sample annealed at  $(500)^\circ\text{C}$  has minimum dislocation density this can attributed to its minimum crystallite size of this sample.

Finally, the number of crystallites per unit area decreases with increasing of  $T_a$ . This result may explained by the mobility of crystallites along the surface of substrate [16]. Fig. (3) shows the variation of transmission ( $T\%$ ) against wavelength. There is no difference in ( $T\%$ ) between that of as deposit and annealed one at  $(300)^\circ\text{C}$ ; this may due to the substrate temperature  $(200)^\circ\text{C}$  at spray time. ( $T\%$ ) of all samples is approximately the same beyond  $(600) \text{ nm}$ . The falling of ( $T\%$ ) toward short wavelength at spectral region of fundamental absorption is sharper for annealed sample at  $(500)^\circ\text{C}$ ; this behavior may relate with the recrystallization at this temperature.



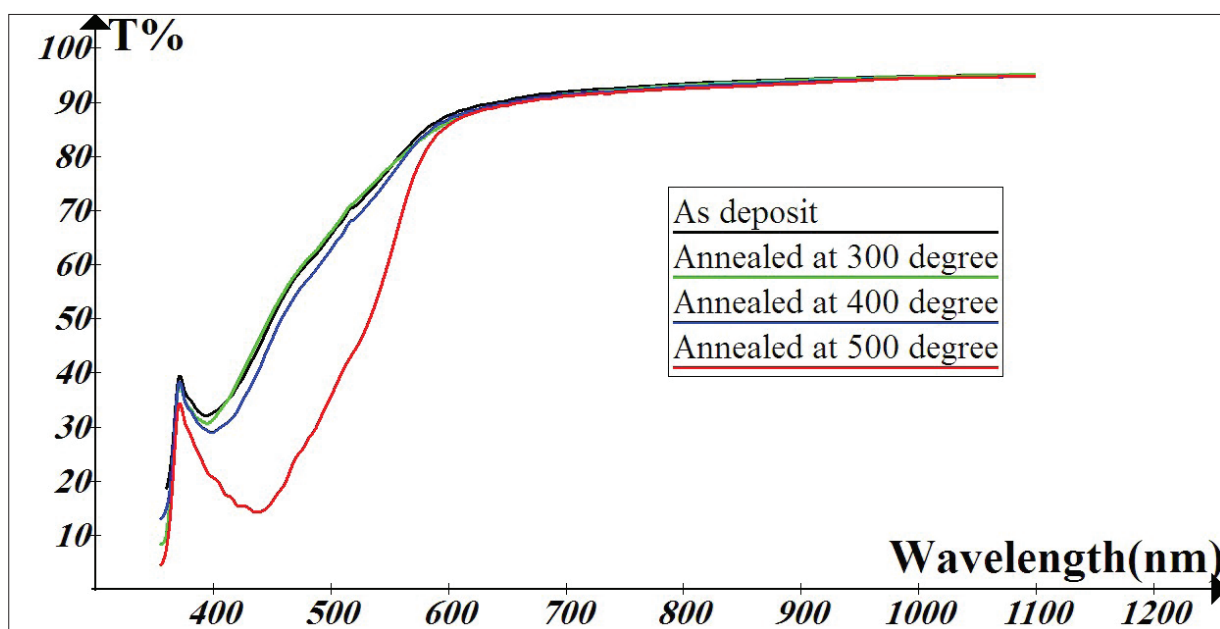


Fig. (3): T % as a function of wavelength for deposit and annealed  $\text{Fe}_2\text{O}_3$  thin films.

For all samples (except that annealed at (500) °C there is no sharp absorption near absorption edge; this is attributed to the existence of sub-band gap levels which relate with defects. This result is expected due the minimum dislocation density of annealed sample at (500) °C as in Table (3). Fig. (4) shows the evaluation of energy gap ( $E_g$ ) values for all samples. Table (4) shows the values of  $E_g$ .

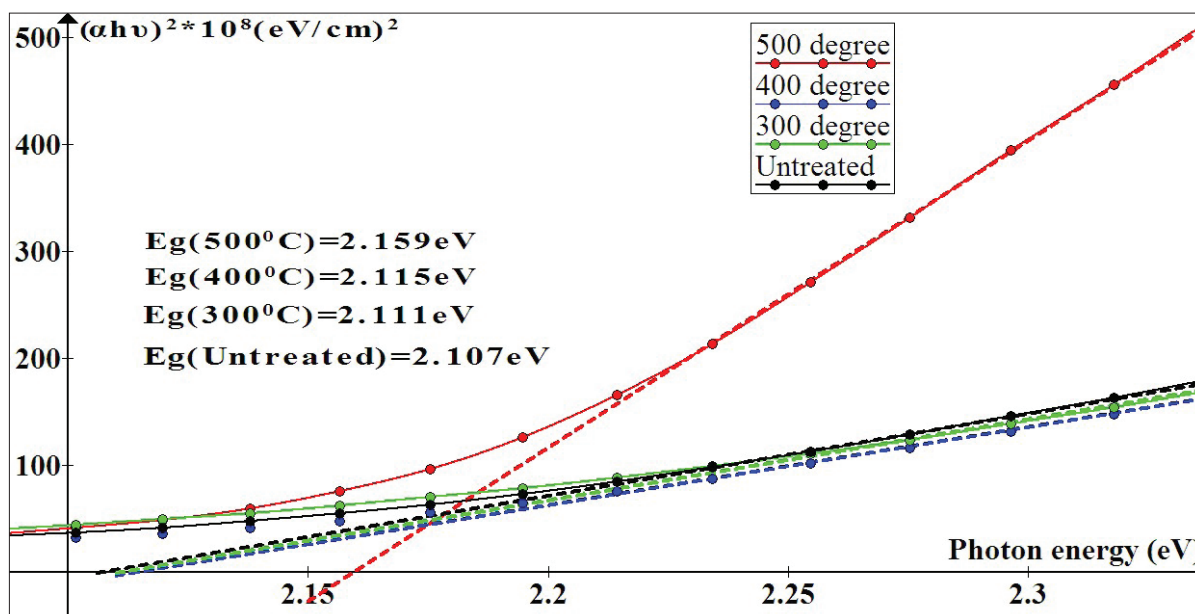


Fig. (4): energy gap ( $E_g$ ) values for deposit and annealed samples.



**Table (4): Eg values for all samples.**

Sample type	Eg (eV)
As deposit	2.107
Annealed at (300) °C	2.111
Annealed at (400) °C	2.115
Annealed at (500) °C	2.159

The Eg values increase with Ta; this is attributed to decreasing of energy levels inside energy gap that relates with defects and dislocations [17]. Fig. (5.A) illustrates relation between  $\ln \alpha$  and photon energy for as deposit and annealed  $\text{Fe}_2\text{O}_3$  thin films, where

$\alpha$  is absorption coefficient. With increasing of Ta localized states in the band gap decrease as Fig. (5.B) shown. This result explains the increasing of Eg in Fig. (4) This result is in agreement with that obtained by Mubarak *et al.* [18]

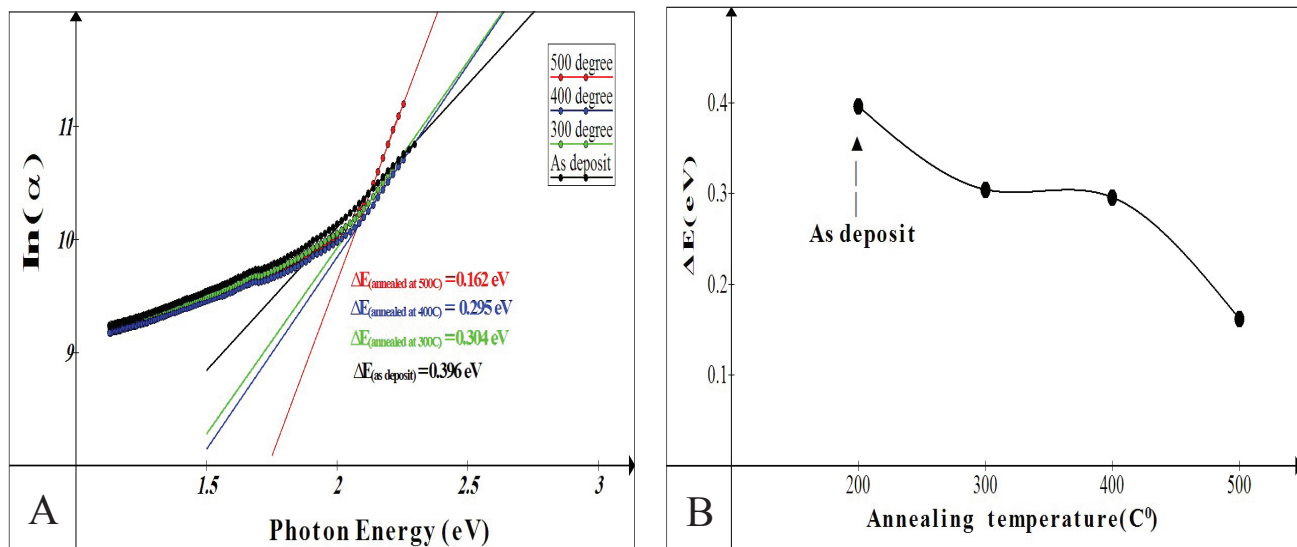


**Fig. (5): A-Determination of localized states width ( $\Delta E$ ) (band tail energy or Urbach energy). B-  $\Delta E$  verses Ta.**

Fig. (6) shows the variation of  $\alpha$  with photon energy. It is clear that the absorption coefficient increases with increasing of Ta and slightly shifted to lower photon energies. The

high values of  $\alpha$  refer to the allowed direct transition for all thin films. This result is in agreement with that obtained by Khalid [19].



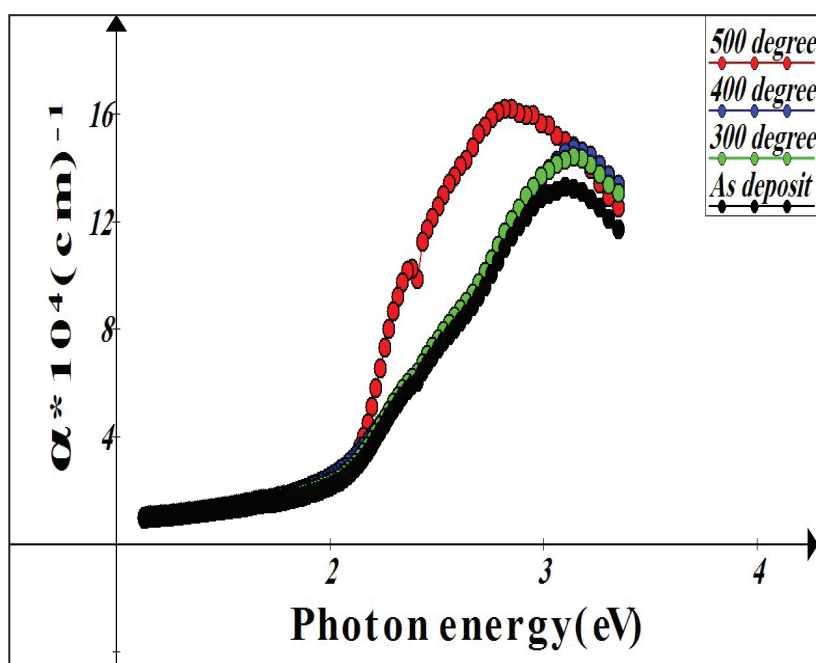


Fig. (6): absorption coefficient variation with photon energy.

#### 4. Conclusions:

Increasing of Ta changed structural and optical properties of  $\text{Fe}_2\text{O}_3$  thin film; crystallite sizes are increased and the crystallinity of it is improved. The annealing process reduces dislocation density and the number of crystallites per unit area but it enhances the micro strain. The  $E_g$  and the absorption coefficient values increase with annealing due to decreasing of localized states in the band gap.

#### References:

- [1] P., Mallick, and B. N. Dash. Nanoscience and nanotechnology. 3(5),130-134, (2013).
- [2] Song, Ha-Chul, Seong-Hun Park and Young-Duk Huh. Bull. Korean Chem. Soc. 28(3), 477-480, (2007).
- [3] Siroky, Karel, Jana Jirešová and Lubomír Hudec. 245(1-2), 211-214, (1994).
- [4] Kennedy, J.H. and D.J.Dunnwald. Electrochem. Soc. 130, 2013-2016, (1983).
- [5] Hahn, Nathan T., Heechang Ye, David W Flaherty, Allen J Bard and C Buddie Mullins. Acs Nano. 4 (4),1977-1986, (2010).
- [6] Akl, A., Applied Surface Science 221,319-329, (2004).
- [7] Seeber, W.T., M.O. Abou-Helal, S. Barth, D. Beil, T. Höche, H.H. Afify, and S.E. Demian. Materials Science in Semiconductor Processing. 2 (1), 45-55, (1999).
- [8] Mishjil, Kh., Asaad A. Kamil and Ahmed N. Jasim. Diyala journal for pure sciences.11(3),1-13, (2015).
- [9] Saini, Isha, Rozra, J., Chandak, N., Aggarwal, S., Sharma, P. K. and Sharma A. Materials Chemistry and Physics 139(2-3),802-810, (2013).
- [10] Jandow, N., Iraqi journal of applied physics,IJAP. 10 (3),17-22, (2014).
- [11] Mitra, P., and Khan, J. Materials Chemistry and Physics. 98(2-3), 279-284, (2008).
- [12] Shinde, S. S., R. A. Bansode, C. H. Bhosale, and K. Y. Rajpure. Journal of Semiconductors. 32(1),1-8, (2011).
- [13] Kariper, I. Afsin. J mater res technol.5(1),77-83,



(2016).

- [14] Berkum, J. G. Van, A. C. Varmcuch, R. Delhen, Th. H. Dinkeijser, and E. J. Hemeijer. J. Appl. Crys. 27,345-357, (1994).
- [15] Sarma, H., Dhruba Chakrabortty and K.C. Sarma. International Journal of Innovative Research in Science Engineering and Technology. 3 (10),16957- 16964, (2014).
- [16] Givargizov, E.I., Oriented crystallization on amorphous substrates, springer science, (1990).
- [17] Habobi, N. Fadel, Reem S.Kh.and Muhammad H.A. Proceeding of 6 th Sci. of Karbala University. (2010).
- [18] Mubarak, T.H., M. H. Abdul-Allah and W.H. Abass. J. of education college, 3, 161-168, (2012).
- [19] Abass,Kh. Haneen. International Letters of Chemistry, Physics and Astronomy. 6,24-31, (2015).